

Precision Orbit Derived Atmospheric Density: Development and Performance

Craig A. McLaughlin, Andrew Hiatt, Dhaval Mysore Krishna, Travis Lechtenberg, Eric Fattig, Piyush M. Mehta

University of Kansas

ABSTRACT

Precision orbit ephemerides (POE) are used to estimate atmospheric density along the orbits of CHAMP (Challenging Minisatellite Payload) and GRACE (Gravity Recovery and Climate Experiment). The densities are calibrated against accelerometer derived densities and considering ballistic coefficient estimation results. The 14-hour density solutions are stitched together using a linear weighted blending technique to obtain continuous solutions over the entire mission life of CHAMP and through 2011 for GRACE. POE derived densities outperform the High Accuracy Satellite Drag Model (HASDM), Jacchia 71 model, and NRLMSISE-2000 model densities when comparing cross correlation and RMS with accelerometer derived densities.

1. INTRODUCTION

The goal of this research is to show the potential for utilizing precision orbit data from a satellite in order to generate corrections to a given density model thus yielding a more accurate density necessary for enhanced atmospheric drag calculations, improved orbit determination and prediction, and an increased understanding and measurement of the density and its variations in the thermosphere and exosphere. Atmospheric density modeling is one of the greatest uncertainties in the dynamics of satellites in low Earth orbit and accurate density calculations are required to generate meaningful estimates of the atmospheric drag perturbing satellite motion.

Reference [1] gives an introduction to the neutral atmosphere and the time varying effects on the thermospheric and exospheric density. These time varying effects include solar rotation, solar cycle, diurnal variations, magnetic storms and substorms, gravity waves, winds and tides, and long-term climate change. Reference [2] gives an introduction to the basic variations in density as well as the most commonly used density models in orbit determination. Reference [3] gives a summary of the drivers of atmospheric density variations as well as discusses some of the difficulties connected with the temporal resolution of various proxies utilized by the empirical density models. Reference [4] supplies an overview of research addressing the inaccuracies in modeling satellite drag.

Two primary categories of research exist to address the problems of modeling atmospheric density for satellite drag. The first category is dynamic calibration of the atmosphere (DCA) and the second is using accelerometers onboard satellites to measure non-conservative accelerations, which includes drag. DCA utilizes the observed motions of a large number of satellites in order to estimate large-scale density corrections to a given atmospheric density model. References [5], [6], [7], [8], [9], [10], [11], and [12] are examples of the DCA approach of making large-scale corrections to existing atmospheric density models. Dynamic calibration of the atmosphere provides a significant improvement to empirical density models but with several disadvantages. First, a DCA approach is designed to run internal to a particular orbit determination scheme with the resulting atmospheric density corrections only applying to a specific time period. Therefore, those using a different orbit determination scheme must rely on that particular system for updates to atmospheric density corrections as well as requiring a complete archive of density corrections for a given problem. The second limitation of DCA approaches is the limited spatial and temporal resolution of the atmospheric density corrections. The corrections allow the baseline density model to characterize atmospheric density variations in terms of several hours to days but not in shorter time scales. A temporal limitation is introduced by the use of a daily solar flux and averaged 3-hour geomagnetic indices as input values into a DCA scheme. The use of this input data does not permit the baseline atmospheric density model to properly represent variations that occur within the averaging interval of these indices. Further difficulty arises in DCA approaches because of the predominate use of two-line element sets of a large number of low Earth orbit objects as observational inputs for a given DCA approach. Reliance on two-line elements results in reduced accuracy density corrections with restricted temporal resolution. The High Accuracy Satellite Drag Model (HASDM) utilizes radar observations of low Earth orbit objects, but the accuracy of radar observations is still lower than those obtained by precision orbit ephemerides (POE) or satellite laser ranging (SLR). In addition, the radar observation data are not generally available.

The second category of research for improving atmospheric density knowledge is using accelerometers onboard satellites to measure non-conservative accelerations, which can be utilized to estimate density. The accelerometer data allows the separation of gravitational forces from non-conservative forces including Earth radiation pressure, solar radiation pressure, and drag. Use of accurate radiation pressure models permits the drag acceleration and resulting estimated density to be accurately calculated with precise temporal resolution. The accelerometer data are extremely precise but only available for a few satellites. This represents an extreme opposite in terms of accuracy and data availability compared with the use of two-line element sets. The availability of accelerometer measurements is recently limited to the Challenging Mini-Satellite Payload (CHAMP) and the two Gravity Recovery and Climate Experiment (GRACE) satellites. Other satellites with accelerometers have flown in the past. An example is given in [13] where the accelerometer data from the Satellite Electrostatic Triaxial Accelerometer (SETA) experiment flown at an altitude of about 200 km was used to examine thermospheric density and confirmed that energy from magnetic storms deposited at high latitudes created a “density bulge” that propagated toward the equator and then toward the opposite poles.

References [14] and [15] published some of the early results for estimating density using CHAMP accelerometer data with additional atmospheric density values derived using CHAMP accelerometer data by [16], [17], and [18]. Reference [19] examined polar region density structures by using CHAMP accelerometer data. Joint work between researchers at the University of Colorado and the Centre National d’Études Spatiales (CNES) utilized CHAMP and GRACE accelerometer data to examine density variations created during solar and geomagnetic events in [20], [21], [22], [23], [24], and [25]. Reference [26] describes a technique to estimate atmospheric density from the GRACE accelerometer data. The CHAMP and GRACE satellites have contributed vast amounts of information regarding the upper atmosphere and are capable of adding even more. Unfortunately, these three satellites only provide limited spatial coverage at any given time and only at low altitudes.

The research presented in this paper is another step toward the goal of combining accurate data with good spatial coverage obtained from a large number of satellites. Many satellites currently possess Global Positioning System (GPS) receivers that when combined with precision orbit determination provide position accuracies of a few centimeters to within a few meters. This research estimates atmospheric density by using the precision orbit data of these satellites in a precision orbit determination scheme. For this research CHAMP and GRACE POEs are used to estimate atmospheric density. Use of POE data results in increased accuracy from a smaller number of satellites as compared with two-line element sets. When compared with accelerometer data, POE data provide a larger number of available satellites with reduced accuracy. Several papers have examined the use of GPS receiver or SLR observations for estimating non-conservative accelerations. One such approach is given in [27], where a type of differential correction was examined by using two-line element sets in a traditional DCA scheme along with a small number of satellites with precision orbit data. Another approach described as GPS accelerometry in [28], [29], and [30], utilizes GPS receiver data to estimate non-conservative forces as empirical accelerations. Through this method the in-track and cross-track accelerations derived from the CHAMP accelerometer may be reasonably determined with a temporal resolution of 20 minutes or greater. Reference [31] utilized batch and Kalman filter estimation techniques in order to investigate the reconstruction of empirical accelerations of the GRACE-B satellite. Both the batch and Kalman techniques demonstrated similar overall variations in the empirical accelerations but with a scale difference between the acceleration magnitudes obtained from the two methods. The research presented here is a summary of all of the analyses performed using the CHAMP and GRACE POE data to estimate density.

2. METHODOLOGY

The results presented in this paper were generated by processing the positions from the CHAMP and GRACE POE data as observations in an orbit determination process in order to estimate density and ballistic coefficient. The POE data are available as rapid science orbits (RSO) and may be downloaded from the website <http://isdc.gfz-potsdam.de>. References [32], [33], [34] and [35] discuss the processing and accuracy of the RSOs. The published accuracy of the RSOs compared to SLR data is 5-10 cm.

Atmospheric density is estimated as a correction to a baseline atmospheric density model as part of an orbit determination scheme. The POE data are input as measurements into a sequential measurement processing and filtering scheme. A smoother is then applied to the filtered solution to account for all available solution data to increase the accuracy over the whole solution span. The filter and smoother combination estimates the time variable

density and ballistic coefficient including realistic covariance matrices established by the physics associated with the problem. A 90x90 GRACE Gravity Model 2 (GGM02C), solar radiation pressure, Earth infrared and albedo radiation pressure, luni-solar point masses, general relativity, and solid Earth and ocean tides are additional force models included in the orbit determination process.

References [36] and [37] outline techniques for estimating density that are available in the Orbit Determination Tool Kit (ODTK) software package. The technique permits the local atmospheric density to be estimated in real-time in conjunction with the orbit determination process and provides a significant improvement over the standard technique of estimating the ballistic coefficient (BC) or drag coefficient because BC estimates absorb the errors generated by the model for atmospheric density and BC. Additionally, BC estimates will often include geopotential model errors. Reference [38] presents the polynomial spline fit technique used to smooth the geomagnetic indices utilized in the orbit determination scheme.

The estimated atmospheric density is obtained as a correction to an atmospheric model. The models available in ODTK are Jacchia 1971, Jacchia-Roberts, CIRA 1972, MSISE-1990, and NRLMSISE-2000. The Jacchia-Roberts and CIRA 1972 density models were derived from the Jacchia 1971 model so the results from these three models should be similar. Once a baseline atmospheric density model is selected, two different types of corrections are applied to the model as part of the orbit determination process. The first is a baseline correction derived from historical F10.7 and a_p measurements obtained over several solar cycles. The baseline density correction propagates from perigee height through the use of an exponential Gauss-Markov sequence. A transformation exists such that the error in the atmospheric density at perigee is related to the current point in the orbit.

The second type of atmospheric density correction utilizes the observations and current conditions to yield a dynamic correction. The use of a sequential process allows a correction to be estimated at each time step in the filter as opposed to a single correction applied to the complete time span of data as for a batch least squares process. Exponentially correlated Gauss-Markov processes describing the modeling errors also exist for dynamic corrections as observed for the baseline corrections. The user of the optimal orbit determination process may specify the values of the density and ballistic coefficient exponential Gauss-Markov process half-lives, which determines the effect of past data on the individual density correction at each time step. While the ballistic coefficient is estimated as part of the filter/smoothing process, the ballistic coefficient for CHAMP was initialized using yearly averages of 0.00444 m^2/kg for 2002-2003 and 0.00436 m^2/kg for 2004-2005 as determined in [39]. These values are used to initialize the satellite in the orbit determination process, in which ballistic coefficient is estimated. Dates not in the given values are extrapolated based on changes in the satellite's mass. The ballistic coefficient for GRACE is initialized as 0.00687 m^2/kg .

The derived densities obtained from the POE data are compared against those derived from the CHAMP accelerometer as calculated by Sean Bruinsma of CNES. Bruinsma's density values are averaged to 10-second intervals. POE derived density solutions were developed for multiple time periods with varying levels of solar and geomagnetic activity. The authors have used geomagnetic and solar activity bins based on [40] to establish low solar activity as defined by $F10.7 < 75$, moderate solar activity for $75 \leq F10.7 < 150$, elevated solar activity for $150 \leq F10.7 < 190$, and high solar activity by $F10.7 \geq 190$. Additionally, quiet geomagnetic periods are defined for $A_p \leq 10$, moderate geomagnetic activity for $10 < A_p < 50$, and active geomagnetic periods by $A_p \geq 50$. These definitions are applied to separate the POE derived density solutions into the appropriate categories. This cataloging of solutions facilitates the analysis of the POE derived density solutions as a function of solar and geomagnetic activity.

3. INITIAL CHAMP RESULTS AND CALIBRATION

Reference [41] presented the initial results of estimating density using CHAMP POE. The paper found densities estimated using different baseline density models and densities estimated in overlap regions to be consistent within 10 percent. Reference [42] made the first comparisons of CHAMP POE derived atmospheric densities to those derived from the accelerometer data and found errors bounded within about 10 percent for days with moderate solar and geomagnetic activity. Follow-on work focused on calibrating the POE derived densities using the accelerometer derived densities. References [43], [44], [45], and [46] presented initial calibration results for CHAMP and showed that density and ballistic coefficient half-lives of 1800 and 180,000 minutes did not perform well in estimating density. Therefore, further work focused on half-lives of 1.8, 18, or 180 minutes. These works also showed that

POE derived corrections to Jacchia based density models matched the accelerometer derived densities better than POE derived corrections to MSIS based density models did. Reference [47] included the most comprehensive examination of CHAMP POE derived densities and examined days from 2001 to 2007 picked so that the distribution of solar and geomagnetic activity level bins matched those over all days from the launch of CHAMP through 2007 and so that days from different times in the year were adequately represented. The results of this study are summarized in Table 1 including the best density half-life, ballistic coefficient half-life, and baseline density model combination. The best combination was determined based on both cross correlation and RMS. Generally, the Jacchia based density models had nearly identical results, especially for cross correlation.

Table 1. Best Combinations for CHAMP POE-Derived Density Correlation and RMS with Accelerometer-Derived Density

Bin	Density Half-Life (min)	BC Half-Life (min)	Atmospheric Model	Cross Correlation	RMS (10^{-12} kg/m ³)
Overall	180	1.8	CIRA 1972	0.910	0.570
Quiet Geomagnetic	180	1.8	CIRA 1972	0.955	0.348
Moderate Geomagnetic	180	1.8	CIRA 1972	0.919	0.464
Active Geomagnetic	18	1.8	CIRA 1972	0.856	0.960
Low Solar	180	1.8	CIRA 1972	0.931	0.296
Moderate Solar	180	1.8	CIRA 1972	0.893	0.559
Elevated Solar	18	1.8	CIRA 1972	0.947	0.581
Active Solar	180	1.8	CIRA 1972	0.906	0.759

These results show the very high correlation between CHAMP POE and accelerometer derived densities and relatively low RMS differences. The consistently best combination included a ballistic coefficient half-life of 1.8 minutes and a CIRA 1972 baseline density model. In addition, 180 minutes was usually the best half-life for density. The differences between density found with 18 and 180 minute half-lives for density was usually negligibly different.

4. CHAMP AND GRACE CALIBRATION

References [48], [49], and [50] presented the first extensive calibration that examined the same days for CHAMP and GRACE to see if the best parameters were consistent between CHAMP and GRACE. These studies included days from when GRACE was launched in 2004 through 2009. No elevated or high solar activity days occurred during this time period. Table 2 shows a summary of the results for CHAMP and Table 3 shows a summary of the GRACE results.

Tables 2 and 3 show that the results are fairly consistent between the CHAMP and GRACE orbits and across solar and geomagnetic activity levels. Again the overall best combination was with corrections to a Jacchia-based model. Ballistic coefficient half-life was best at 1.8 minutes and the density half-life was best at 18 or 180 minutes with the difference between the densities estimated with the two density half-lives being small.

Table 2. Best Combinations for CHAMP POE-Derived Density Correlation and RMS with Accelerometer-Derived Density

Bin	Density Half-Life (min)	BC Half-Life (min)	Atmospheric Model	Cross Correlation	RMS (10^{-12} kg/m ³)
Overall	18	1.8	CIRA 1972	0.883	0.623
Quiet Geomagnetic	180	1.8	CIRA 1972	0.936	0.272
Moderate Geomagnetic	180	1.8	CIRA 1972	0.945	0.418
Active Geomagnetic	18	1.8	CIRA 1972	0.818	0.961
Low Solar	180	1.8	CIRA 1972	0.928	0.264
Moderate Solar	18	1.8	CIRA 1972	0.868	0.761

Table 3. Best Combinations for GRACE POE-Derived Density Correlation and RMS with Accelerometer-Derived Density

Bin	Density Half-Life (min)	BC Half-Life (min)	Atmospheric Model	Cross Correlation	RMS (10^{-12} kg/m ³)
Overall	180	1.8	Jacchia-Roberts	0.849	0.123
Quiet Geomagnetic	180	1.8	Jacchia 1971	0.802	0.037
Moderate Geomagnetic	180	1.8	Jacchia-Roberts	0.912	0.076
Active Geomagnetic	180	1.8	Jacchia-Roberts	0.845	0.207
Low Solar	180	1.8	Jacchia 1971	0.766	0.030
Moderate Solar	180	1.8	Jacchia-Roberts	0.883	0.160

References [51] and [52] examined the simultaneous ballistic coefficient and density estimation. The estimated density magnitude is sensitive to the nominal ballistic coefficient selected so a bias in nominal ballistic coefficient does lead to a bias in the estimated density. Therefore, ballistic coefficient and density are not completely separable without a good knowledge of what the average ballistic coefficient should be. The estimated ballistic coefficients show a 3-5% percent variation in magnitude with a cycle of roughly twice per orbit. For CHAMP, the correlation between the density error, defined as the difference between accelerometer and POE derived densities, and the ballistic coefficient was around -0.3 for ballistic coefficient half-life of 1.8 min and density half-life of 18 min and near zero if density half-life was increased to 180 min. For GRACE the correlation for the density half-life of 180 min was 0.1 with other results about the same as for CHAMP. If ballistic coefficient error was being absorbed by the density estimation, one would expect a high negative correlation between these two quantities. However, some ballistic coefficient error is almost certainly being absorbed in the density estimates, but the effects on the density estimation appear to be small based on comparisons with the accelerometer. These papers also examined the effects of fixing ballistic coefficient at the nominal value and showed that the difference in density is small between estimating and not estimating the ballistic coefficient.

Based on the density and ballistic coefficient studies, nominal settings were used for further analysis. The nominal settings were to use CIRA 1972 as the baseline density model, ballistic coefficient half-life of 1.8 minutes, and density half-life of 180 minutes. An additional benefit of 180 minute half-life compared to the 18 minute half-life is that it provides an additional order of magnitude difference between the ballistic coefficient and density half-lives. Large separation between density and ballistic coefficient half-lives was a condition for the two factors to be simultaneously observable.

5. CONTINUOUS DENSITY DATA SETS AND ACCURACY COMPARISONS

References [53] and [54] present the technique used to combine 14 hour density solutions into a continuous density data set over the life of CHAMP and from launch through 2011 for GRACE. The data are available as one week data sets to keep the individual file sizes manageable. The method used to merge the data is the linear weighted blending technique, which appears in [55], [56], and [57]. The technique applies weights to overlapping areas of the fourteen day density solution based on how far the point is from the end or beginning of the overlapping solution. The 14 hour solutions have two hour overlaps so at the beginning of the two hour overlap the combined density will match the density of the earlier of the two fourteen hour solutions; at the midpoint of the overlap region the combined density will be a straight average of the two densities; and at the end of the overlap region the combined density will match the density of the latter of the two fourteen hour solutions. This primary value of this technique is to provide a smooth solution, but it also gives more weight to points farthest from the endpoint of a given solution. This is valuable since for an orbit solution one would typically expect the points at the end of a given solution to be of lower accuracy than points closer to the middle. Effectively, this technique uses information from the other overlapping solution to provide more information about what is happening in the overlap regions.

Cross correlation and RMS between HASDM, POE derived, and Jacchia 71 densities with accelerometer derived densities were calculated and compared for both CHAMP and GRACE. Table 4 contains the cross correlation coefficients of the POE derived density, HASDM densities, and of the Jacchia 71 model compared to accelerometer

derived density for the various levels of solar and geomagnetic activity as well as for the entire mission life. The RMS comparisons are contained in Table 5. The tables show the POE derived density is significantly better than Jacchia 71 and gets more so as solar activity increases. The POE derived density is also moderately better than the HASDM density. CHAMP is included as a satellite in the HASDM solutions so the HASDM densities for CHAMP are likely better than for a satellite not included in the HASDM solutions.

Table 4. Cross correlation coefficients for POE derived density, HASDM, and Jacchia 71 with accelerometer derived density along the CHAMP orbit.

Bin	Cross Correlation		
	HASDM	POE derived density	Jacchia-71
Overall	0.924	0.934	0.886
Low Solar	0.910	0.926	0.884
Moderate Solar	0.925	0.935	0.884
Elevated Solar	0.936	0.938	0.895
High Solar	0.942	0.948	0.895
Quiet Geomagnetic	0.923	0.935	0.896
Moderate Geomagnetic	0.924	0.932	0.874
Active Geomagnetic	0.941	0.950	0.831

Table 5. RMS for POE derived density, HASDM, and Jacchia 71 with accelerometer derived density along the CHAMP orbit.

Bin	Root Mean Square (10^{-12} kg/m ³)		
	HASDM	POE derived density	Jacchia-71
Overall	0.400	0.383	0.836
Low Solar	0.346	0.322	0.925
Moderate Solar	0.372	0.354	0.663
Elevated Solar	0.531	0.526	1.027
High Solar	0.576	0.573	1.434
Quiet Geomagnetic	0.361	0.346	0.759
Moderate Geomagnetic	0.441	0.423	0.895
Active Geomagnetic	0.986	0.925	3.231

Table 6 shows the cross correlation and Table 7 shows the RMS results for GRACE. No elevated or high solar activity days or active geomagnetic weeks occurred during the available GRACE POE data (starting in 2004). The trends are very similar to those observed in the CHAMP data. Once again the POE derived density is clearly superior to the Jacchia 71 model and slightly better than HASDM in matching the accelerometer derived density. These results show the promise of POE derived density from many satellites to improve the overall knowledge of density in the thermosphere.

Table 6. Cross correlation coefficients for POE derived density, HASDM, and Jacchia 71 with accelerometer derived density along the GRACE orbit.

Bin	Cross Correlation		
	HASDM	POE derived density	Jacchia-71
Overall	0.873	0.885	0.839
Low Solar	0.840	0.855	0.816
Moderate Solar	0.902	0.912	0.859
Quiet Geomagnetic	0.869	0.883	0.840
Moderate Geomagnetic	0.881	0.891	0.836

Fig. 1 shows the cross correlation of CHAMP POE derived and HASDM densities with accelerometer derived densities and the angle between the CHAMP orbit plane and the Sun vector, β , from 2001 to 2008. Fig. 2 shows the same for GRACE. Both figures show a periodic variation in correlation for both POE and HASDM densities where the lower correlation occurs where β is near zero. This occurs when the orbit plane is near the terminator. The reason for the lower correlation is that the normal daylight/darkness variation that dominates the signal is much

lower in amplitude when the orbit plane is near the terminator. When this happens the high frequency density variations that are only observed by the accelerometer are of the same order as the daylight/darkness variations, which brings the correlations down. This is discussed more fully in [58].

Table 7. RMS for POE derived density, HASDM, and Jacchia 71 with accelerometer derived density along the GRACE orbit.

Bin	Root Mean Square (10^{-12} kg/m ³)		
	HASDM	POE derived density	Jacchia-71
For all Bins	0.047	0.044	0.111
Low Solar	0.031	0.031	0.100
Moderate Solar	0.060	0.056	0.122
Quiet Geomagnetic	0.038	0.036	0.096
Moderate Geomagnetic	0.068	0.063	0.147

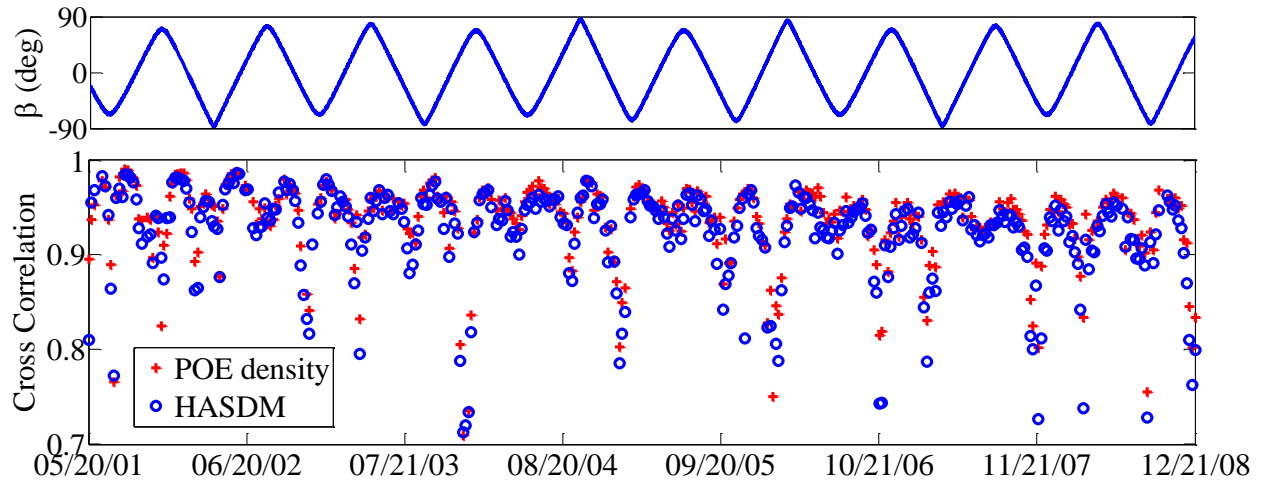


Fig. 1. Beta angle and weekly cross correlation between POE and HASDM densities with accelerometer densities for CHAMP

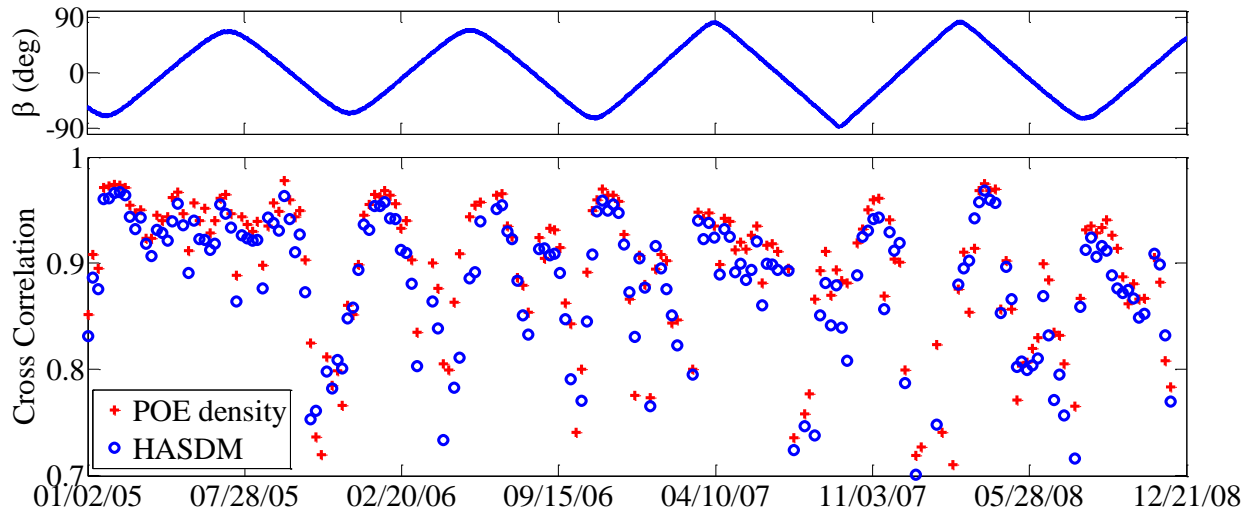


Fig. 2. Beta angle and weekly cross correlation between POE and HASDM densities with accelerometer densities for GRACE

6. CONCLUSIONS

Precision orbit ephemeris (POE) data are used as measurements in an orbit determination process to estimate neutral atmospheric density along the CHAMP and GRACE orbits. The combination of CIRA 1972 as a baseline density model with ballistic coefficient half-life of 1.8 minutes and density half-life of 180 minutes was found to be the overall combination for estimating POE derived densities that best matched accelerometer derived densities as measured by cross correlation and RMS.

POE derived densities were found for the entire life of CHAMP and from launch through 2011 for GRACE. The density data exists as a continuous data set divided into one week files for ease of access. The POE derived densities were shown to better match, in terms of cross correlation and RMS, the accelerometer derived densities than either HASDM or Jacchia 71 density models. The cross correlation between other density sources and the accelerometer derived densities was lower when the orbit plane of the satellite was near the terminator.

7. ACKNOWLEDGMENTS

This material is based upon work supported by the National Science Foundation under Grant No. 0832900 and by the Department of Defense Experimental Program to Stimulate Competitive Research (DEPSCoR) grant FA9550-10-1-0038 administered by the Air Force Office of Scientific Research. Any opinions, findings, and conclusions or recommendations expressed in this material are those of the authors and do not necessarily reflect the views of NSF or AFOSR. David Vallado provided help with data conversion scripts and working with Orbit Determination Tool Kit. Jens Ramrath provided help with scripting and many other ins and outs of Orbit Determination Tool Kit. Bruce Bowman provided access to HASDM densities along the CHAMP and GRACE orbits. Sean Bruinsma provided CHAMP and GRACE accelerometer derived densities and helpful advice about this research. Eric Sutton of AFRL figured out the relation between lower correlations and the orbit plane being near the terminator.

8. REFERENCES

1. McLaughlin, C. A., "Upper Atmospheric Phenomena and Satellite Drag," *Advances in the Astronautical Sciences*, Vol. 123, AAS 05-315, Univelt, 2005, pp. 989-996.
2. Vallado, D. A., *Fundamentals of Astrodynamics and Applications*, Microcosm Press, El Segundo, CA, 3rd Edition, 2007, Chap. 8, App. B.
3. Sabol, C., and K. K. Luu, "Atmospheric Density Dynamics and the Motion of Satellites," *AMOS Technical Conference*, Wailea, HI, September 2002.
4. F. O. Marcos, J. O. Wise, M. J. Kendra, and N. J. Grossbard, "Satellite Drag Research: Past, Present, and Future," *Advances in the Astronautical Sciences*, Vol. 116, AAS 03-620, Univelt, 2003, pp. 1865-1878.
5. Storz, M. F., Bowman, B. R., Branson, J. I., Casali, S. J., and Tobiska, W. K., "High Accuracy Satellite Drag Model (HASDM)," *Advances in Space Research*, Vol. 36, No. 12, 2005, pp. 2497-2505.
6. Bowman and M. F. Storz, "High Accuracy Satellite Drag Model (HASDM) Review," *Advances in the Astronautical Sciences*, Vol. 116, AAS 03-625, Univelt, 2003, pp. 1943-1952.
7. Bowman, B., F. A. Marcos, and M. J. Kendra, "A Method for Computing Accurate Atmospheric Density Values from Satellite Drag Data," *Advances in the Astronautical Sciences*, Vol. 119, AAS 04-173, Univelt, 2004, pp. 1117-1134.
8. Cefola, P. J., R. J. Proulx, A. I. Nazarenko, and V. S. Yurasov, "Atmospheric Density Correction Using Two Line Element Sets as the Observation Data," *Advances in the Astronautical Sciences*, Vol. 116, AAS 03-626, Univelt, 2003, pp. 1953-1978.
9. Yurasov, V. S., A. I. Nazarenko, P. J. Cefola, and K. T. Alfriend, "Results and Issues of Atmospheric Density Correction," *Journal of the Astronautical Sciences*, Vol. 52, No. 3, July-September 2004, pp. 281-300.
10. Yurasov, V. S., A. I. Nazarenko, K. T. Alfriend, and P. J. Cefola, "Reentry Time Prediction Using Atmospheric Density Corrections," *Journal of Guidance, Control, and Dynamics*, Vol. 31, No. 2, March-April 2008, pp. 282-289.
11. Wilkins, M. P., C. A. Sabol, P. J. Cefola, and K. T. Alfriend, "Improving Dynamic Calibration of the Atmosphere," *Advances in the Astronautical Sciences*, Vol. 127, AAS 07-185, Univelt, 2007, pp. 1257-1272.
12. Wilkins, M. P., C. A. Sabol, P. J. Cefola, and K. T. Alfriend, "Validation and Application of Corrections to the NRLMSISE-00 Atmospheric Density Model," *Advances in the Astronautical Sciences*, Vol. 127, AAS 07-189, Univelt, 2007, pp. 1285-1304.

13. Rhoden, E. A., J. M. Forbes, and F. A. Marcos, "The Influence of Geomagnetic and Solar Variability on Lower Thermospheric Density," *Journal of Atmospheric and Solar-Terrestrial Physics*, Vol. 62, 2000, pp. 999-1013.
14. König, R. and K. H. Neumayer, "Thermospheric Events in CHAMP Precise Orbit Determination," *First CHAMP Mission Results for Gravity, Magnetic and Atmospheric Studies*, eds. C. Reigber, H. Luhr, P. Schwintzer, Springer, Berlin, 2003, pp. 112-119.
15. Bruinsma, S., and R. Biancale, "Total Density Retrieval with STAR," *First CHAMP Mission Results for Gravity, Magnetic and Atmospheric Studies*, eds. C. Reigber, H. Luhr, P. Schwintzer, Springer, Berlin, 2003, pp. 192-199.
16. Bruinsma, S., and R. Biancale, "Total Densities Derived from Accelerometer Data," *Journal of Spacecraft and Rockets*, Vol. 40, No. 2, March-April 2003, pp. 230-236.
17. Bruinsma, S., S. D. Tamagnan and R. Biancale, "Atmospheric Densities Derived from CHAMP/STAR Accelerometer Observations," *Planetary and Space Science*, Vol. 52, 2004, pp. 297-312.
18. Nerem, R. S., J. M. Forbes, E. K. Sutton, and S. Bruinsma, "Atmospheric Density Measurements Derived from CHAMP/STAR Accelerometer Data," *Advances in the Astronautical Sciences*, Vol. 116, AAS 03-621, Univelt, 2003, pp. 1879-1898.
19. Schlegel, K., H. Luhr, J. P. St. Maurice, G. Crowley, and C. Hackert, "Thermospheric Density Structures over the Polar Regions Observed with CHAMP," *Annales Geophysicae*, Vol. 23, 2005, pp. 1659-1672.
20. Sutton, E. K., R. S. Nerem, and J. M. Forbes, "Global Thermospheric Neutral Density and Wind Response to the Severe 2003 Geomagnetic Storms from CHAMP Accelerometer Data," *Journal of Geophysical Research*, Vol. 110, 2005.
21. Forbes, J. M., G. Lu, S. Bruinsma, S. Nerem, and X. Zhang, "Thermospheric Density Variations Due to the 15-24 April 2002 Solar Events from CHAMP/STAR Accelerometer Measurements," *Journal of Geophysical Research*, Vol. 110, 2005, pp. 1-9.
22. Sutton, E. K., J. M. Forbes, R. S. Nerem, and T. N. Woods, "Neutral Density Response to the Solar Flares of October and November, 2003," *Geophysical Research Letters*, Vol. 33, 2006.
23. Bruinsma, S., J. M. Forbes, R. S. Nerem, and X. Zhang, "Thermospheric Density Response to the 20-21 November 2003 Solar and Geomagnetic Storm from CHAMP and GRACE Accelerometer Data," *Journal of Geophysical Research*, Vol. 111, No. AO6303, 2006, pp. 1-14.
24. Bruinsma S. L., and J. M. Forbes, "Storm-Time Equatorial Density Enhancements Observed by CHAMP and GRACE," *Journal of Spacecraft and Rockets*, Vol. 44, No. 6, 2007, pp. 1154-1159.
25. E. K. Sutton, R. S. Nerem, and J. M. Forbes, "Density and Winds in the Thermosphere Deduced from Accelerometer Data," *Journal of Spacecraft and Rockets*, Vol. 44, No. 6, 2007, pp. 1210-1219.
26. Tapley, B. D., J. C. Ries, S. Bettadpur, and M. Cheng, "Neutral Density Measurements for the Gravity Recovery and Climate Experiment Accelerometers," *Journal of Spacecraft and Rockets*, Vol. 44, No. 6, 2007, pp. 1220-1225.
27. Doornbos, E., H. Klinkrad, and P. Visser, "Atmospheric Density Calibration Using Satellite Drag Observations," *Advances in Space Research*, Vol. 36, 2005, pp. 515-521.
28. van den Ijssel, J., P. Visser, and R. Haagmans, "Determination of Non-Gravitational Accelerations from Orbit Analysis," *Earth Observation with CHAMP Results from Three Years in Orbit*, eds. C. Reigber, H. Luhr, P. Schwintzer, J. Wickert, Springer, Berlin, 2005, pp. 95-100.
29. van den Ijssel, J., and P. Visser, "Determination of Non-Gravitational Accelerations from GPS Satellite-to-Satellite Tracking of CHAMP," *Advances in Space Research*, Vol. 36, 2005, pp. 418-423.
30. van den Ijssel, J., and P. Visser, "Performance of GPS Accelerometry: CHAMP and GRACE," *Advances in Space Research*, Vol. 39, 2007, pp. 1597-1603.
31. Montenbruck, O., T. van Helleputte, R. Kroes, and E. Gill, "Reduced Dynamic Orbit Determination Using GPS Code and Carrier Measurements," *Aerospace Science and Technology*, Vol. 9, 2005, pp. 261-271.
32. König, R., S. Zhu, C. Reigber, K. H. Neumayer, H. Meixner, R. Galas, G. Baustert, "CHAMP Rapid Orbit Determination for GPS Atmospheric Limb Sounding," *Advances in Space Research*, Vol. 30, No. 2, 2002, pp. 289-293.
33. König, R., G. Michalak, K. H. Neumayer, S. Y. Zhu, H. Meixner, C. Reigber, "Recent Developments in CHAMP Orbit Determination at GFZ," *Earth Observation with CHAMP Results from Three Years in Orbit*, eds. C. Reigber, H. Luhr, P. Schwintzer, J. Wickert, Springer, Berlin, 2005, pp. 65-70.
34. König, R., G. Michalak, K. H. Neumayer, S. Zhu, "Remarks on CHAMP Orbit Products," *Observation of the Earth System from Space*, eds. J. Flury, R. Rummel, C. Reigber, M. Rothacher, G. Boedecker, U. Schreiber, Springer, Berlin, 2006, pp. 17-26.

35. Michalak, G., G. Baustert, R. Konig, C. Reigber, "CHAMP Rapid Science Orbit Determination: Status and Future Prospects," *First CHAMP Mission Results for Gravity, Magnetic and Atmospheric Studies*, eds. C. Reigber, H. Luhr, P. Schwintzer, Springer, Berlin, 2003, pp. 98-103.
36. Wright, J. R., "Real-Time Estimation of Local Atmospheric Density," *Advances in the Astronautical Sciences*, Vol. 114, AAS 03-164, Univelt, 2003, pp. 927-950.
37. Wright, J. R., and J. Woodburn, "Simultaneous Real-Time Estimation of Atmospheric Density and Ballistic Coefficient," *Advances in the Astronautical Sciences*, Vol. 119, AAS 04-175, Univelt, 2004, pp. 1155-1184.
38. Tanygin, S., and J. R. Wright, "Removal of Arbitrary Discontinuities in Atmospheric Density Modeling," *Advances in the Astronautical Sciences*, Vol. 119, AAS 04-176, Univelt, 2004, pp. 1185-1196.
39. Bowman, B. R., F. A. Marcos, K. Moe, M. M. Moe, "Determination of Drag Coefficient Values for CHAMP and GRACE Satellites Using Orbit Drag Analysis," *Advances in the Astronautical Sciences*, Vol. 129, AAS 07-259, Univelt, 2008, pp. 147-166.
40. Picone, J. M., A. E. Hedin, D. P. Drob, "NRLMSISE-00 Empirical Model of the Atmosphere: Statistical Comparisons and Scientific Issues," *Journal of Geophysical Research*, Vol. 107, No. A12, 2002.
41. McLaughlin, C. A., and B. S. Bieber, "Neutral Density Determined from CHAMP Precision Orbits," *Astrodynamics 2007*, Vol. 129 of *Advances in the Astronautical Sciences*, AAS 07-260, 2007, pp. 167-186.
42. McLaughlin, C. A., A. Hiatt, and B. S. Bieber, "Comparison of Total Density Derived from CHAMP Precision Orbits and CHAMP Accelerometer," *Space Flight Mechanics 2008*, Vol. 130 of *Advances in the Astronautical Sciences*, AAS 08-177, 2008, pp. 1193-1206.
43. McLaughlin, C. A., A. Hiatt, and T. Lechtenberg, "Calibrating Precision Orbit Derived Total Density," *AIAA/AAS Astrodynamics Specialist Conference*, Honolulu, HI, AIAA 2008-6951, 18-21 August 2008.
44. McLaughlin, C. A., A. Hiatt, and T. Lechtenberg, "Precision Orbit Derived Total Density," *Journal of Spacecraft and Rockets*, Vol. 48, No. 1, January-February 2011, pp. 166-174.
45. Hiatt, A., C. A. McLaughlin, and T. Lechtenberg, "Deriving Density Estimates Using CHAMP Precision Orbit Data for Periods of High Solar Activity," *Space Flight Mechanics 2009*, Vol. 134 of *Advances in the Astronautical Sciences*, 2009, AAS 09-104, pp. 23-42.
46. Hiatt, A., "Deriving Atmospheric Density Estimates Using Satellite Precision Orbit Ephemerides," M. S. Thesis, Department of Aerospace Engineering, University of Kansas, 2009.
47. T. Lechtenberg, "Derivation and Observability of Upper Atmospheric Density Variations Utilizing Precision Orbit Ephemerides," M. S. Thesis, Department of Aerospace Engineering, University of Kansas, 2010.
48. Fattig, E., McLaughlin, C. A., and T. Lechtenberg, "Comparison of Density Estimation for CHAMP and GRACE Satellites," *AIAA/AAS Astrodynamics Specialist Conference*, Toronto, ON, AIAA 2010-7976, 2-5 August 2010.
49. McLaughlin, C. A., T. Lechtenberg, E. Fattig, D. Mysore Krishna, "Estimating Density Using Precision Satellite Orbits from Multiple Satellites," *Journal of the Astronautical Sciences*, (in press).
50. Fattig, E., "Comparison of Precision Orbit Derived Density Estimates for CHAMP and GRACE Satellites," M. S. Thesis, Department of Aerospace Engineering, University of Kansas, 2011.
51. McLaughlin, C. A., A. Hiatt, E. Fattig, and T. Lechtenberg, "Ballistic Coefficient and Density Estimation," *Astrodynamics 2009*, Vol. 135 of *Advances in the Astronautical Sciences*, 2009, AAS 09-439, pp. 2269-2285.
52. Mehta, P. M. and C. A. McLaughlin, "Density and Ballistic Coefficient Estimation Revisited," *Astrodynamics 2011*, Vol. 142 of *Advances in the Astronautical Sciences*, 2011, AAS 11-609, pp. 3247-3264.
53. Mysore Krishna, D., and C. A. McLaughlin, "Combining Precision Orbit Derived Density Estimates," *Astrodynamics 2011*, Vol. 142 of *Advances in the Astronautical Sciences*, 2011, AAS 11-475, pp. 3229-3246.
54. Mysore Krishna, D., "Improving and Expanding Precision Orbit Derived Atmospheric Densities" M. S. Thesis, Department of Aerospace Engineering, University of Kansas, 2012.
55. Kim, J., "Bridging methods for the JB2006 and NRLMSISE-00 thermospheric density models in the altitude range of 140 km through 200 km," M. S. Thesis, Department of Aerospace Engineering, Pennsylvania State University, August, 2008.
56. Kim, J., D. B. Spencer, T. J. Kane, J. Urbina, "A blending technique in thermospheric density modeling," *AIAA/AAS Astrodynamics Specialist Conference and Exhibit*, AIAA, Honolulu, Hawaii, 18-19 August, 2008.
57. Kim, J., D. B. Spencer, T. J. Kane, J. Urbina, "Thermospheric density model blending techniques: Bridging the gap between satellites and sounding rockets," *Radio Science*, Vol. 44, RSO 22, 2009.
58. McLaughlin, C. A., E. Fattig, D. Mysore Krishna, T. Locke, and P. M. Mehta, "Time Periods of Anomalous Density for CHAMP and GRACE," *Astrodynamics 2011*, Vol. 142 of *Advances in the Astronautical Sciences*, 2011, AAS 11-613, pp. 3299-3310.